

Competition between Electromagnetically Induced Transparency and Raman Processes

G. S. Agarwal* and T. N. Dey†

Department of Physics, Oklahoma State University, Stillwater, Oklahoma 74078, USA

Daniel J. Gauthier

Department of Physics, Duke University, Durham, North Carolina, 27708, USA

(Dated: July 10, 2018)

We present a theoretical formulation of competition among electromagnetically induced transparency (EIT) and Raman processes. The latter become important when the medium can no longer be considered to be dilute. Unlike the standard formulation of EIT, we consider all fields applied and generated as interacting with both the transitions of the Λ scheme. We solve Maxwell equations for the net generated field using a fast-Fourier-transform technique and obtain predictions for the probe, control and Raman fields. We show how the intensity of the probe field is depleted at higher atomic number densities due to the build up of multiple Raman fields.

PACS numbers: 42.50.Gy, 42.65.-k

Multilevel atomic system interacting with several electromagnetic fields can give rise to variety of phenomena that depend on the strength and detunings of the fields. Often, the various processes compete with each other, whereby some processes are suppressed or interference between processes renders the medium transparent to the applied fields [1]. Well known examples include competition between third-harmonic generation and multiphoton ionization [2], and four-wave mixing and two-photon absorption [3, 4]. Very recently, Harada *et al.* demonstrated experimentally that stimulated Raman scattering can disrupt electromagnetically induced transparency (EIT), where the incident probe beam is depleted and new fields are generated via Raman processes [5]. The disruption of EIT is important to understand because it may degrade the performance of EIT-based applications, such as optical memories and buffers, and magnetometers. In this paper we present a theoretical formulation that enables us to study the competing EIT and various orders of Raman processes to all orders in the applied and generated fields.

The standard treatment of EIT [6] is based on the scheme of Fig. 1, where the atoms in the state $|c\rangle$ interact with a probe field of frequency ω . A control field of frequency ω_c interacts on the unoccupied transition $|a\rangle \leftrightarrow |b\rangle$. The probe and the control fields are tuned such that

$$\omega - \omega_c = \omega_{bc}. \quad (1)$$

This results in no absorption of the probe field provided the coherence ρ_{bc} has no decay. This treatment assumes that the frequency separation ω_{bc} is so large that the interaction of the control field ω_c (probe field ω) with

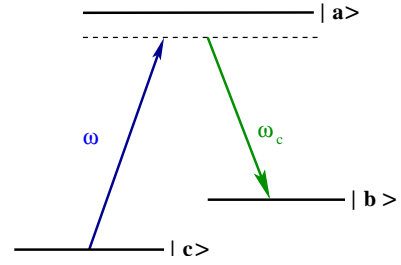


FIG. 1: (Color online) A schematic diagram of a three-level atomic system with energy spacing $\hbar\omega_{bc}$ between two ground states $|c\rangle$ and $|b\rangle$. The control field with frequency ω_c and probe field with frequency ω act on the atomic transitions $|a\rangle \leftrightarrow |b\rangle$ and $|a\rangle \leftrightarrow |c\rangle$, respectively.

the transition $|a\rangle \leftrightarrow |b\rangle$ ($|a\rangle \leftrightarrow |c\rangle$) can be ignored. At high atomic number densities or for strong fields, this approximation no longer holds, which is the situation we consider here.

At higher densities, Raman processes start becoming important [7, 8], such as those shown in the Fig 2, for example. The Raman generation of the fields at $\omega_c - \omega_{bc}$, $\omega + \omega_{bc}$ can further lead to newer frequencies like $\omega_c - 2\omega_{bc}$. In order to account for the Raman processes, we write the electromagnetic field acting on both the transitions as

$$E(t) = \mathcal{E}(t)e^{-i\omega_c t}, \quad (2)$$

where $\mathcal{E}(t)$ denotes the net generated field. At the input face of the medium $\mathcal{E}(t)$ has two components to account for both control and probe fields

$$\mathcal{E}(t) = \mathcal{E}_c + \mathcal{E}_p e^{-i(\omega - \omega_c)t}. \quad (3)$$

Under the Raman-resonance condition (1), we expect $\mathcal{E}(t)$ to have the structure

$$\mathcal{E}(t) = \sum \mathcal{E}^{(n)} e^{-in\omega_{bc}t}. \quad (4)$$

*On leave of absence from Physical Research Laboratory, Navrangpura, Ahmedabad - 380 009, India.

†Electronic address: tarak.dey@okstate.edu

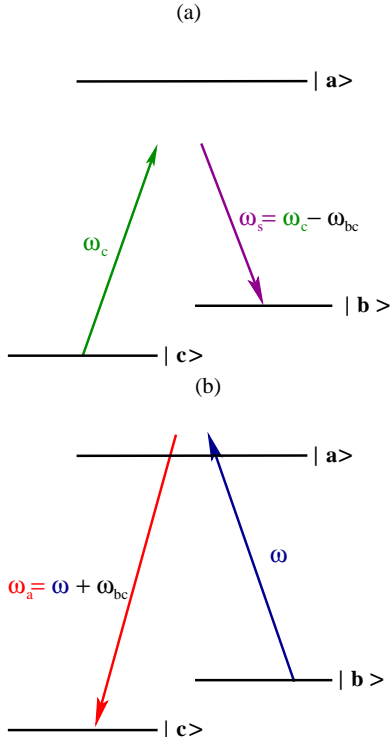


FIG. 2: (Color online) Diagrammatic explanation of the (a) Stokes and (b) anti-Stokes processes. The intermediate state is denoted by $|a\rangle$.

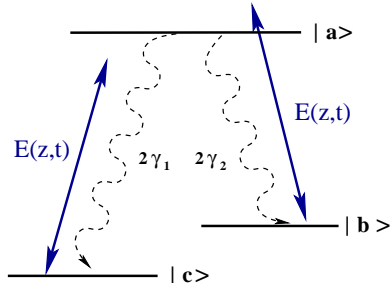


FIG. 3: (Color online) Three-level Λ system interacting with the space-time dependent field $E(z,t)$ on both the optical transitions.

Thus, $\mathcal{E}^{(-1)}$ gives the strength of the Stokes process of the Fig. 2(a); $\mathcal{E}^{(+2)}$ gives the strength of the process of the Fig. 2(b); and $\mathcal{E}^{(+1)}$ describes the changes in the probe field. For low atomic number densities, we expect the usual results and therefore $\mathcal{E}^{(+1)} \approx \mathcal{E}$ and $\mathcal{E}^{(0)} \approx \mathcal{E}_c$.

To calculate the net generated field $\mathcal{E}(t)$ for arbitrary atomic number density, we have to solve the coupled Maxwell and density matrix equations. We consider now the situation as shown schematically in the Fig. 3. The applied field $E(z,t)$ couples the excited state $|a\rangle$ to both ground states $|b\rangle$ and $|c\rangle$. Here 2γ 's represents rates

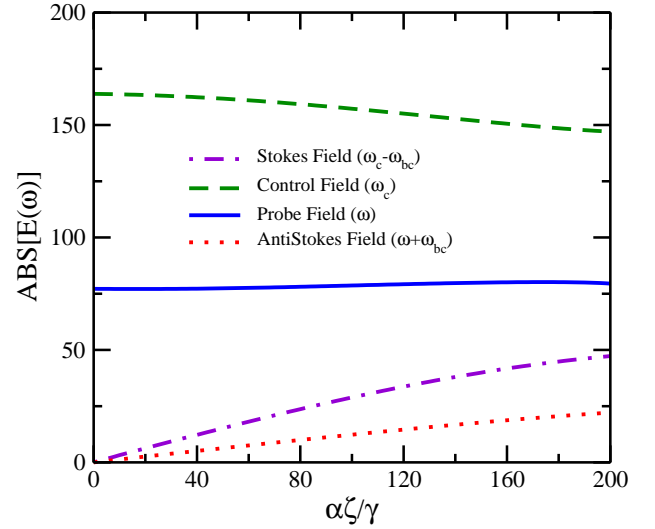


FIG. 4: (Color online) Amplitudes of different Fourier components of the net generated field as a function of the atomic density of the medium. The normalized propagation length $\alpha\zeta/\gamma = 200$ is equivalent to actual length of the medium $L=7.13$ cm with an atomic density of $n = 10^{10}$ atoms/cm³. The other parameters of the above graph are chosen as: input Rabi frequency $\Omega_{\mathcal{E}} = 0.5\gamma$, $\mathcal{E}_p/\mathcal{E}_c = 0.5$, $\Delta_c = 0.0$, $\gamma = 9.475 \times 10^6$, $\Gamma_{bc} = 0.0$, $\omega_{bc} = 100\gamma$ and $\lambda = 766.4$ nm.

of spontaneous emission. In a frame rotating with the frequency ω_c the density matrix equation for the atomic system are given by

$$\begin{aligned} \dot{\rho}_{aa} &= i\Omega_{\mathcal{E}}(\rho_{ba} + \rho_{ca}) - i\Omega_{\mathcal{E}}^*(\rho_{ab} + \rho_{ac}) - 4\gamma\rho_{aa}, \\ \dot{\rho}_{bb} &= i\Omega_{\mathcal{E}}\rho_{ab} - i\Omega_{\mathcal{E}}\rho_{ba} + 2\gamma\rho_{aa}, \\ \dot{\rho}_{ab} &= -[2\gamma - i\Delta_c]\rho_{ab} + i\Omega_{\mathcal{E}}(\rho_{bb} - \rho_{aa}) + i\Omega_{\mathcal{E}}\rho_{cb}, \\ \dot{\rho}_{ac} &= -[2\gamma - i(\Delta_c - \omega_{bc})]\rho_{ac} + i\Omega_{\mathcal{E}}\rho_{bc} + i\Omega_{\mathcal{E}}(\rho_{cc} - \rho_{aa}), \\ \dot{\rho}_{bc} &= -(\Gamma_{bc} + i\omega_{bc})\rho_{bc} + i\Omega_{\mathcal{E}}^*\rho_{ac} - i\Omega_{\mathcal{E}}\rho_{ba}, \end{aligned} \quad (5)$$

where the detuning Δ_c and the space and time dependent Rabi frequency $\Omega_{\mathcal{E}}$ of the generated fields are defined by

$$\Delta_c = \omega_c - \omega_{ac}; \quad \Omega_{\mathcal{E}}(z,t) = \frac{\vec{d} \cdot \vec{\mathcal{E}}}{\hbar}. \quad (6)$$

For simplicity, we have assumed $\vec{d}_{ab} = \vec{d}_{ac} = \vec{d}$. The elements ρ_{ac} and ρ_{ab} in the original frame can be obtained by multiplying the solution of Eqs. (5) by $e^{-i\omega_c t}$. The induced polarization $\vec{\mathcal{P}}$ is given by

$$\vec{\mathcal{P}} = \left(\vec{d}\rho_{ab} + \vec{d}\rho_{ac} \right) e^{-i\omega_c t}. \quad (7)$$

The Maxwell equations in the slowly varying envelope approximation lead to the following equation for the generated field

$$\left(\frac{\partial \Omega_{\mathcal{E}}}{\partial z} + \frac{\partial \Omega_{\mathcal{E}}}{\partial ct} \right) = i\frac{\alpha}{2}(\rho_{ac} + \rho_{ab}), \quad (8)$$

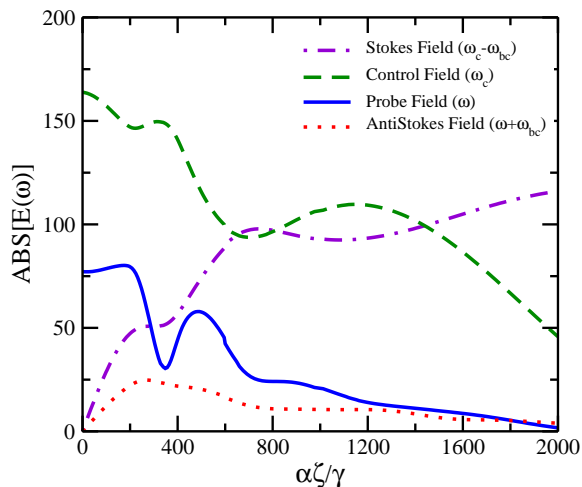


FIG. 5: (Color online) The spectral amplitudes of different fields are plotted against the atomic density of the medium. The normalized propagation length $\alpha\zeta/\gamma = 2000$ is equivalent to actual length of the medium $L=7.1$ cm when the atomic density $n = 10^{11}$ atom/cm³. The other parameters are chosen as: input Rabi frequency $\Omega_{\mathcal{E}} = 0.5\gamma$, $\mathcal{E}_p/\mathcal{E}_c = 0.5$, $\Delta_c = 0.0$, $\Gamma_{bc} = 0.0$ and $\omega_{bc} = 100\gamma$.

where α is given by

$$\alpha = 3\lambda^2 n \gamma / 4\pi, \quad (9)$$

and n is the atomic density. The coupled equations (5) and (8) are solved in the moving coordinate system

$$\tau = t - \frac{z}{c}; \quad \zeta = z. \quad (10)$$

We have numerically solved the coupled set of equations when all the atoms are initially in the state $|c\rangle$ and when the fields at the input face of the medium are given by (3). We calculate $\mathcal{E}(l, \tau)$ and do a fast Fourier transform to obtain the different Fourier components of the field at the output face of the medium. This procedure enables us to find how the probe and control fields evolve and determine when the Raman processes become important. In the simulations, we have used parameters that are appropriate for ³⁹K vapor [8] to avoid numerical problems. In this situation, the spontaneous decay rate of the excited state $|a\rangle$ $4\gamma = 3.79 \times 10^7$ rad/s and the wavelength for the ground state $|c\rangle$ to excited state $|a\rangle$ transition $\lambda = 766.4$ nm.

EIT Vs Raman Processes In this section, we present the results of numerical calculations. In Fig. 4, we show result for the low-density regime. In this region, we notice almost no change in the probe field and thus EIT dominates. It is also seen that the Raman processes slowly start to build up, leading to the drop in the control field amplitude.

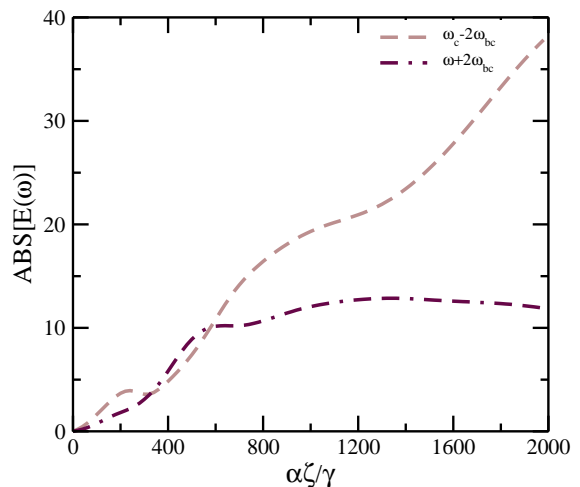


FIG. 6: (Color online) The amplitudes of hyper Raman components at frequencies $(\omega_c - 2\omega_{bc})$, $(\omega + 2\omega_{bc})$ as a function of the atomic density. All parameters are same as in Fig. (5).

We next consider the high-density regime, as shown in Fig. 5. This is the region when multiple Raman processes build up significantly [9]. Our numerical results are in broad agreement with the observations of Harada *et al.*[5] where they observe the depletion of the probe field and the generation of the Stokes field at $(\omega_c - \omega_{bc})$. In particular, we see in fig. 5 that the generation of radiation at $(\omega_c - \omega_{bc})$ is very important and the probe beam is depleted. We also notice a new feature - the probe exhibits some oscillatory character before dying out. This oscillation is due to the fact that any population that is transferred to the state $|b\rangle$ can produce a field at the probe frequency via the Raman process. When this happens, the control field amplitude falls.

In Fig. 6, we show the build up of several hyper-Raman processes. The effect of a buffer gas on the generated field is shown in Fig. 7, where it is seen that the amplitude of the probe field depletes faster in the presence of buffer gas. On comparison of Fig. 5 and Fig. 7, we see that the amplitudes of the probe field and the generated Raman field become equal at $\alpha\zeta/\gamma = 272$ (without buffer gas) and 84 (with buffer gas). This is in agreement with the observation in Ref.[5].

In conclusion, we have investigated competition between electromagnetically induced transparency and Raman processes in a Λ system due to the cross talk among the optical transitions. We have demonstrated that the EIT-induced probe spectrum is very pronounced in comparison to the higher order Raman sidebands for a low atomic number density. However, the generated Raman fields become dominant for an atomic number density that is only ten times higher.

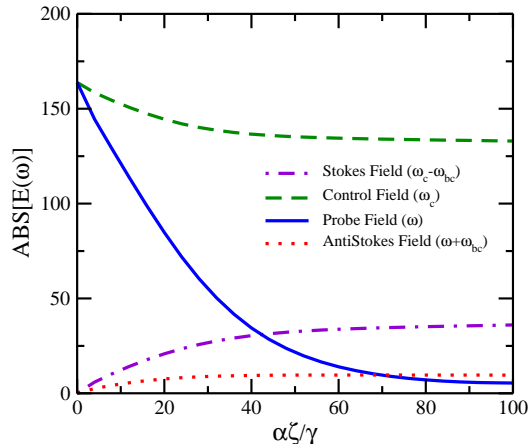


FIG. 7: (Color online) The amplitudes of Stokes, control, probe and anti-Stokes fields as a function of the atomic number density in the presence of a buffer gas. Here, we have scaled the amplitudes of probe, Stokes and anti-Stokes fields by a factor of two. The other parameters are chosen as: density $n = 10^{10}$ atom/cm³, input Rabi frequency $\Omega_{\mathcal{E}} = 0.5\gamma$, $\mathcal{E}_p/\mathcal{E}_c = 0.5$, $\Delta_c = 0.0$, $\Gamma_{bc} = 0.01\gamma$ and $\omega_{bc} = 100\gamma$. A nonzero value of Γ_{bc} accounts for the buffer gas.

-
- [1] D.J. Gauthier, J. Chem. Phys. **99**, 1618 (1993).
[2] S.P. Tewari and G.S. Agarwal, Phys. Rev. Lett. **56**, 1811 (1986) and references therein.
[3] M. S. Malcuit, D. J. Gauthier, and R. W. Boyd, Phys. Rev. Lett. **55**, 1086 (1985); R. W. Boyd, M. S. Malcuit, D. J. Gauthier, and K. Rzażewski Phys. Rev. A **35**, 1648 (1987).
[4] G. S. Agarwal, Phys. Rev. Lett. **57**, 827 (1986).
[5] K. I. Harada, T. Kanbashi, M. Mitsunaga and K. Motomura, Phys. Rev. A **73**, 013807 (2006). These authors examine their experiments using an analysis based on linearized equations for probe and Stokes fields and no depletion of the control field. In our work we treat all fields on equal basis as the depletion of the control field could be important and several higher order Raman processes become active
[6] S. E. Harris, J. E. Field, and A. Imamoglu, Phys. Rev. Lett. **64**, 1107 (1990); S.E. Harris, Phys. Today **50**(7), 36 (1997).
[7] M. Poelker and P. Kumar, Opt. Lett. **17**, 399 (1992); M. Poelker, P. Kumar, and S.-T. Ho, Opt. Lett. **16**, 1853 (1991); M. T. Gruneisen, K. R. MacDonald, and R. W. Boyd, J. Opt. Soc. Am. B **5**, 123 (1988); P. Kumar and J. H. Shapiro, Opt. Lett. **10**, 226 (1985).
[8] H.M. Concannon, W.J. Brown, J.R. Gardner, and D.J. Gauthier, Phys. Rev. A **56**, 1519 (1997).
[9] The generation of multiple Raman sidebands has been considered under the condition that the excited state is far detuned from any of the exciting frequencies; A. V. Sokolov, D. D. Yavuz, and S. E. Harris, Opt. Lett. **24** 557 (1999); K. Hakuta, M. Suzuki, M. Katsuragawa, and J.Z Li, Phys. Rev. Lett. **79**, 209 (1997). Furthermore, Raman generation in a coherently prepared medium has been considered by A. F. Huss, N. Peer, R. Lammeggar, E. A. Korsunsky, and L. Windholz, Phys. Rev. A **63**, 013802 (2000).